ORIGINAL ARTICLE

Simulation of ice formation by the finite volume method

Rotchana Prapainop[1] and Kuntinee Maneeratana[2]

Abstract

Prapainop, R. and Maneeratana, K.
Simulation of ice formation by the finite volume method
Songklanakarin J. Sci. Technol., 2004, 26(1) : 55-70

This paper investigates the simulation of ice formation in one and two dimensions by the cell-centred finite volume method. The model is based on the heat conduction equation with the fixed grid, latent heat source approach. The piecewise-linear profile of variables in space is employed. For the temporal discretisation, three time-stepping schemes are compared: the explicit, Crank-Nicolson, and the fully implicit schemes. Also examined are different approximations of conductivity at interfaces between adjacent ice and water control volumes, i.e. the 2 well established arithmetic and harmonic means of ice and water conductivities; while the use of ice conductivity is introduced. It is found that numerical results of all temporal schemes show excellent agreements with analytical solutions and exhibit similar accuracies once grid and time interval independencies are achieved. The explicit scheme, however, has superior CPU-time efficiency. For the investigation on the interface conductivity, the conductivity approximation as that of ice yields the most accurate computed temperature field.

Key words : phase change, fixed grid, latent heat, finite volume method

[1]B.Eng.(Mechanical Engineering), Graduate Student, [2]Ph.D., DIC (Mechanical Engineering), Department of Mechanical Engineering, Faculty of Engineering, Chulalongkorn University, Phaya Thai Road, Bangkok 10330 Thailand
Corresponding e-mail: kuntinee.m@chula.ac.th
Received, 13 November 2002 Accepted, 14 October 2003

บทคัดย่อ

รจนา ประไพนพ และ กุณฑินี มณีรัตน์

การจำลองแบบการขึ้นรูปของน้ำแข็งด้วยระเบียบวิธีไฟไนต์วอลุม

ว. สงขลานครินทร์ วทท. 2547 26(1) : 55-70

งานวิจัยนี้เสนอการจำลองแบบของการเปลี่ยนสถานะจากน้ำเป็นน้ำแข็งในหนึ่งและสองมิติ โดยระเบียบวิธีไฟไนต์วอลุมแบบเซลล์เซนเตอร์ โดยมีสมการการนำความร้อนเป็นสมการพื้นฐาน และใช้การพิจารณาจุดต่อแบบอยู่กับที่และคำนวณปริมาณความร้อนแฝงจากค่าความร้อนสัมผัสสมมุติ ประมาณตัวแปรให้มีการกระจายตามระยะทางเชิงเส้นตรง และประมาณตัวแปรที่เปลี่ยนแปลงตามเวลาด้วยระบบช่วงเวลาสองชั้น 3 แบบ ได้แก่ แบบชัดแจ้ง แบบแครงค์-นิโคลสัน และแบบปริยาย ส่วนการประมาณค่าสัมประสิทธิ์การนำความร้อนที่รอยต่อใช้ค่าเฉลี่ยแบบธรรมดา 2 รูปแบบ คือ ค่าเฉลี่ยเลขคณิต ค่าเฉลี่ยฮาร์มอนิก และเสนอการใช้สัมประสิทธิ์การนำความร้อนในสถานะของแข็งเพิ่มขึ้นอีกวิธีหนึ่ง ในการพิจารณาการประมาณตัวแปรที่เปลี่ยนแปลงตามเวลา พบว่าผลเฉลยที่ได้จากการประมาณตัวแปรที่เปลี่ยนแปลงตามเวลาทุกวิธีมีค่าใกล้เคียงกัน และใกล้เคียงผลเฉลยแม่นตรงเมื่อขนาดปริมาตรควบคุมและช่วงเวลามีขนาดเล็กจนไม่มีผลต่อผลลัพธ์ที่ได้ จึงพบว่าวิธีแบบชัดแจ้งมีการประมวลผลที่มีประสิทธิภาพสูงสุด และในการพิจารณารูปแบบการประมาณค่าสัมประสิทธิ์การนำความร้อนที่รอยต่อสถานะได้ผลว่า การประมาณค่าสัมประสิทธิ์การนำความร้อนที่รอยต่อสถานะด้วยสัมประสิทธิ์การนำความร้อนในสถานะของแข็ง จะได้ผลเฉลยจากการจำลองแบบที่มีความใกล้เคียงผลเฉลยแม่นตรงมากที่สุด

ภาควิชาวิศวกรรมเครื่องกล คณะวิศวกรรมศาสตร์ จุฬาลงกรณ์มหาวิทยาลัย ถนนพญาไท กรุงเทพฯ 10330

Ice manufacturers for food industries in Thailand have consumed huge amount of electricity in the manufacturing process. Thus, the purpose of this work is to obtain suitable mathematical models and numerical schemes for the development of a simulation program for ice formation, leading to further studies on energy-saving and quality improvements.

Unique features of solidification problems are the continuously moving liquid-solid front and the latent heat that is released on this interface. In addition, the ice formation is an isothermal phase change problem which involves abrupt discontinuity of properties at the constant freezing temperature.

Over the years, a number of related computational works have employed various techniques in the analysis of phase change problems. Table 1 shows the schemes used in selected papers. Previous studies use combinations of two approaches, the grid consideration and the latent heat representation methods.

The grid consideration approach may be further divided into front tracking and fixed grid methods. In the front tracking scheme, favoured by Rubinsky and Cravahlo (1981), Voller and Cross (1981), Voller and Cross (1983), Weaver and Viskanta (1986) and Askar (1987), the position of moving liquid-solid interface is determined in every time step, frequently with immobilised freezing front in transformed coordinates (Kim and Kaviany, 1990). Hence, this method does not require the discontinuity approximation for iso-thermal problems. The main drawback, however, is the extremely complicated calculation of inter-face movements in multi-dimensional modelling.

Thus, many researchers, such as Comini *et al*. (1974), Morgan *et al*. (1978), Roose and Storrer (1984), Dalhuijsen and Segal (1986), Pham (1986), Dhatt *et al*. (1989), Comini *et al*. (1990) and Voller *et al*. (1990), recommend the fixed grid method, which implicitly contains the moving interface condition within the mathematical model. This method is more flexible than the front tracking

Table 1. Comparisons of numerical schemes in selected isothermal phase change papers.

Paper	Method	Grid		Primary variable				Time-stepping			
		Front track	Fixed grid	Temp	Basic *H*	Apparent *h*	Fictitious *h*	Explicit	C-N	Implicit	Two step
Murray & Landis (1959)	FD	●		●							●
Morgan *et al*. (1978)	FE		●			●					●
Lemmon (1979)	FD	●			●			●			
Rubisky & Cravahlo (1981)	FE	●					●	●			
Voller & Cross (1981)	FD	●			●			●			
Rolph & Bathe (1982)	FE		●				●			●	
Voller & Cross (1983)	FD	●			●			●		●	
Roose & Storrer (1984)	FE		●				●				
Pham (1986)	FE		●		●			●			●
Crivelli & Idelsohn (1986)	FE		●	●						●	
Dalhuijsen & Segal (1986)	FE		●			●	●				●
Weaver & Viskanta (1986)	FD	●		●						●	
Askar (1987)	FE	●		●					●		
Dhatt *et al*. (1989)	FE		●		●			●			
Comini *et al*. (1990)	FE		●			●					●
Kim & Kaviany (1990)	FD	●			●			●			
Voller *et al*. (1990)	FE, FV		●	●	●	●	●			●	
Tamma & Namburu (1990)	FE		●			●		●		●	
Celentano *et al*. (1994)	FE		●	●						●	

and is suitable for multi-dimensional problems.

It is noted that in some works, for instance, Weaver and Viskanta (1986), the grid is fixed in most of the domain apart from the moving freezing front in order to eliminate the problematical approximation at the interface. Hence, the computation grid on both sides of the interface changes sizes and careful consideration of temperature gradient is required.

For the second type of approaches, the latent heat is accounted for by either the temperature-based or the enthalpy-based method. The temperature-based approach insists on retaining the temperature as the only state variable. In order to avoid the discontinuity in isothermal problems, an approximate numerical smoothing must be used and a special integration is needed to compute the latent heat (Murray and Landis, 1959; Crivelli and Idelsohn, 1986; Celentano *et al*., 1994).

On the other hand, the enthalpy-based method is further divided into basic enthalpy, apparent heat capacity and latent heat source sub-categories. In the basic enthalpy scheme, enthalpy is used as the primary variable and the temperature is calculated from a previously defined enthalpy-temperature relation. This method gives reasonably accurate results for metallic solidifying over mushy ranges (Thomas *et al*., 1987), but it is complex and computationally expensive. More importantly, it performs poorly for isothermal problems.

In the apparent heat capacity method, the latent heat is calculated from the integration of heat capacity with respect to temperature (Comini

et al., 1974; Morgan *et al*., 1978; Guidice *et al*., 1978; Lemmon, 1979; Tamma and Namburu, 1990). As the relationship between heat capacity and temperature in isothermal problems involves sudden changes, the zero-width phase change interval must be approximated by a narrow range of phase change temperatures. Thus, the size of time steps must be small enough that this temperature range is not overlooked in the calculation.

The drawbacks of previously described enthalpy-based methods are not observed in the latent heat source or fictitious heat flow method. In this approach, the latent heat is included in the source term, which is obtained from a prescribed relationship between latent enthalpy and temperature. If the fully implicit time-stepping scheme is used, e.g. Rolph and Bathe (1982) and Dalhuijsen and Segal (1986), an iterative scheme is used for calculating the latent heat increment.

Comparing the advantages and disadvantages of these approaches for the finite volume simulation, this work chooses the combination of fixed grid and the latent heat source schemes. The proposed latent heat source method is similar to the previously described one, but the latent heat increment is calculated after the computation of fictitious temperature in the freezing region and then the temperature fields are adjusted.

The main objective of this study is the detailed investigations of the effects of different types of interface conductivity approximation and the time-stepping schemes on the accuracy and efficiency of finite volume modelling which were not formally compared in previous works (Table 1). In all, two established interface conductivity approximations are considered, the arithmetic and the harmonic means while the use of solid con-ductivity is proposed. The three time-stepping schemes are explicit, Crank-Nicolson and fully implicit. Then the suitable combination of con-ductivity approximation and time-stepping schemes are chosen for future development.

Mathematical Model

The law of conservation of energy and the Fourier's law of heat conduction are employed. The combined equations can be written in the local form as:

$$\frac{\partial H}{\partial t} = \frac{\partial}{\partial x}(k\frac{\partial T}{\partial x}) + \frac{\partial}{\partial y}(k\frac{\partial T}{\partial y}), \qquad (1)$$

where H, T and k are the enthalpy, temperature and thermal conductivity, respectively, and:

$$H = \int_{T_{ref}}^{T} \rho c_S dT \qquad \text{when } T<T_F,$$

$$H = \int_{T_{ref}}^{T_F} \rho c_S dT + \rho L + \int_{T_F}^{T} \rho c_L dT \qquad \text{when } T\geq T_F, \qquad (2)$$

where ρ is mass density, c is the specific heat, L is the latent heat per unit mass, T_{ref} is the reference temperature and T_F is the freezing temperature. The subscripts S and L indicate the solid and liquid properties, respectively.

Hence, the total latent heat of phase change Q_P^{tot} of each control volume is

$$Q_P^{tot} = \int_v \rho L dv. \qquad (3)$$

It is noted that this work neglects effects of the radiation as well as all modes of convection, e.g. thermal, solidification expansion and bulk convection, as described by Prapainop (2002). Thus, the density of the ice is approximated to that of the water to ensure the conservation of mass due to the lack of mass convection across cell faces.

Finite Volume Formulation

The cell-centered finite volume procedure follows the work by Patankar (1980). The discretisation and distribution of variables are explained. Different approximated models of material properties at the liquid-solid interface are also described. Then, mathematical equations for all control volumes are approximately integrated over time intervals to obtain the numerical solutions.

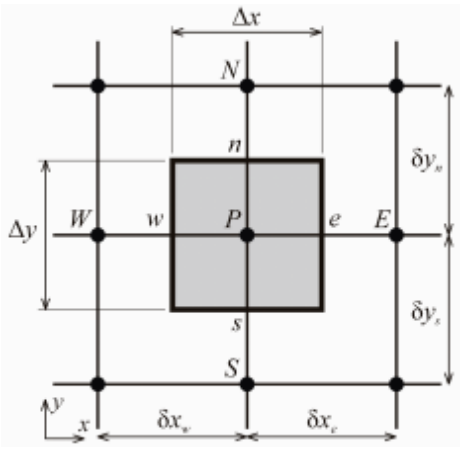

Figure 1. A typical 2D control volume (shaded area).

1. Discretisation of Space and Time

The computational space is divided into a number of non-overlapping control volumes (Figure 1). A typical control volume or cell P is represented by the node P at the centre. The cell P has 4 adjacent neighbours - E, W, N and S with connecting cell faces e, w, n and s. For 2D problems, unit thickness in the z direction is assumed while the 1D problems specify unit width with insulated boundary conditions in the y direction. The location of any variables is indicated by the subscripted position.

The time domain is divided into an arbitrary number of time steps of size t. Variables at time t are indicated by the superscript 0. In contrast, the variables at time level $t+ t$ are not superscripted.

2. Approximations of Distributions in Space

The second-order accurate piecewise-linear temperature profile is assumed for tem-perature. For instance, the temperature at face e is $T_e = T_P f_e + T_E(1-f_e)$ where $f_e = (2\delta x_e - x)/2\delta x_e$.

The other variable that has to be approximated at cell faces is the interface conductivity k_{INT}. This work investigates three types of approximations at a cell face shared by control volumes with different conductivities, k_S for solid and k_L for liquid.

The arithmetic mean is the most straightforward average procedure which assumes a linear variation between two adjacent nodes $k_{INT} = k_{ARITH} = k_P f_e + k_E(1-f_e)$.

The harmonic mean is used for composite materials for its superior handling of abrupt property changes by recognizing that the primary interest is to obtain a good representation of heat flux across interfaces rather than that of the the conductivity (Patankar, 1980):

$$\frac{1}{k_{INT}} = \frac{1}{k_{HAR}} = \frac{1-f_e}{k_P} + \frac{f_e}{k_E}. \qquad (4)$$

As solidification progresses through the saturated control volume, the interfaces between the fully frozen and saturated control volumes are fully frozen most of the time. Hence, the use of solid conductivity at the interface is also proposed such that $k_{INT} = k_S$. In certain sense, the method is analogous to the upwind scheme, in which the upwind property dominates the downwind values.

3. Time-Stepping Schemes

In this study, the temporal distributions of temperature is approximated by two-time level schemes (Versteeg and Malalasekera, 1995) such that:

$$\int_{t}^{t+\Delta t} T dt = [fT - (1-f)T^0]\Delta t, \qquad (5)$$

where f is a weighting factor with the value between 0 and 1.

Three main schemes are considered: explicit, Crank-Nicolson and fully implicit. The first-order accurate explicit method uses temperature gradients of the previous time step t to calculate the unknown T at $t+\ t$ such that $f = 0$. Hence, the time step size $\ t$ is limited to $\ t < \rho c(\ x\ )^2/2k$ for 1D and $\ t < \rho c(\ x^{\ 2}\ y^2)/2k(\ x^{\ 2}+\ y^2)$ for 2D problems. The second-order accurate Crank-Nicolson scheme uses the average of previous and present temperature gradients to compute the present temperature, or $f = 0.5$, and, hence, has less severe step size limitation than the explicit scheme. Meanwhile, The fully implicit scheme is unconditional stable with first-order accuracy as $f = 1$.

4. Approximation of the Mathematical Model

In the calculation, the governing equation is the heat conduction equation (1) without the latent heat term. Whenever a control volume has reached the freezing temperature, sensible heat that are removed from the cells are instead converted to latent heat and the temperature of the control volume is held constant at freezing temperature. This accumulated latent heat is used to indicate the phase status of the control volume. The position of freezing front in the cell is not explicitly calculated in the fixed grid technique. Instead, the saturated control volumes compose of mushy mix of ice and liquid water, whose percentage mass may be calculated from the ratio of accumulated latent heat to total latent heat.

In each time step, governing equation is numerically integrated over the control volume and time as:

$$\int_{t}^{t+\Delta t}\int_{s}^{n}\int_{w}^{e} \rho c \frac{\partial T}{\partial t} dxdydt = \int_{t}^{t+\Delta t}\int_{s}^{n}\int_{w}^{e} \frac{\partial}{\partial x}(k\frac{\partial T}{\partial x})dxdydt + \int_{t}^{t+\Delta t}\int_{s}^{n}\int_{w}^{e} \frac{\partial}{\partial y}(k\frac{\partial T}{\partial y})dxdydt. \qquad (6)$$

For the transient term, it is assumed that the temperature of the control volume is represented by that of the node:

$$\int_{t}^{t+\Delta t}\int_{s}^{n}\int_{w}^{e} \rho c \frac{\partial T}{\partial t} dxdydt \approx \rho c(T_P - T_P^0)\Delta x\Delta y. \qquad (7)$$

The diffusion terms are approximated using the piecewise-linear temperature profile. For instance:

$$\int_{t}^{t+\Delta t}\int_{s}^{n}\int_{w}^{e} \frac{\partial}{\partial x}(k\frac{\partial T}{\partial x})dxdydt \approx [\frac{k_e(T_E - T_P)}{\delta x_e} - \frac{k_w(T_P - T_W)}{\delta x_w}]\Delta y\Delta t. \qquad (8)$$

By substituting the approximated terms in (7) and (8) as well as a time-stepping scheme in section 3.3 into (6), the discretised equation for a control volume P is obtained as:

$$\left(\sum_Q a_Q f + \frac{\rho c\Delta V}{\Delta t}\right)T_P = \sum_Q a_Q[fT_Q + (1-f)T_Q^0] + [\frac{\rho c\Delta V}{\Delta t} - \sum_Q (1-f)a_Q]T_P^0, \qquad (9)$$

where a is the coefficients of the neighbouring nodes and the summation is performed over all neighbouring nodes Q.

5. Solution Algorithm

The overview of the solution algorithm is shown in Figure 2. Prior to the first time interval, the accumulated latent heat of a control volume P,

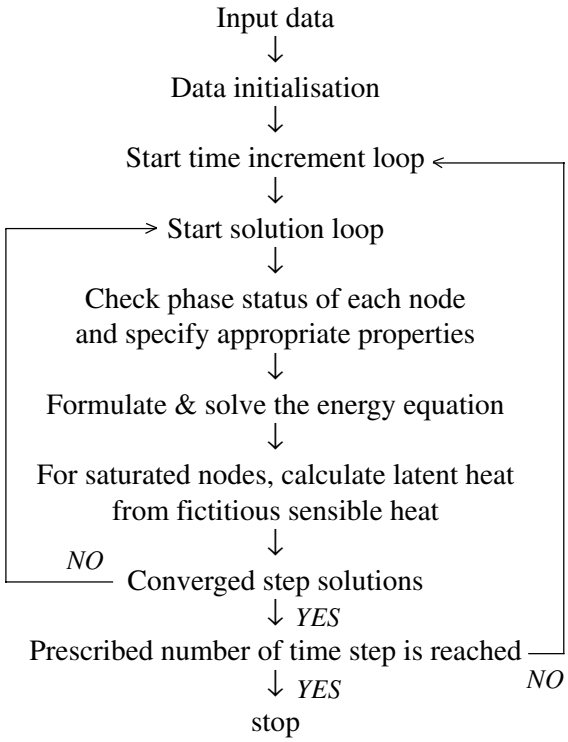

Figure 2. Solution algorithm

Q_P^{lat}, is initialised as zero. At the beginning of each time step, the phase status of each control volume is checked. If the nodal phase is liquid and the previous nodal temperature T_P^0 drops lower than the freezing temperature T_F, the control volume becomes saturated and its node is tagged. Special attentions are due to the cell face conductivity, which depends on the status of the nodal phase.

The nodal temperature is then reassigned to the freezing temperature and the latent heat increment, the energy used for phase change in the current time step, is calculated from the fictitious sensible heat such that $\Delta Q_P^{lat} = \rho c(T_F - T_P)dV$.

The ΔQ_P^{lat} is added to the accumulated Q_P^{lat} for subsequent time steps until the accumulated latent heat equals the total latent heat available at the node. At this stage, the control volume becomes solid, the tag on the cell is removed and the latent heat increment is no longer calculated.

The resulting system of simultaneous equations is assembled and solved with the tri-diagonal matrix algorithm (TDMA) on a personal computer with 733 MHz, Pentium III CPU. The solution of the model with the explicit time-stepping scheme is directly computed from the known nodal temperatures of the previous time interval. For other schemes with f 0, the resulting system of simultaneous equations has to be re-formed and solved until convergence is achieved.

Results and Discussions

After the program is tested for simple transient heat conduction problems, 1D and 2D phase change test cases with analytical solutions are simulated. Then, a real problem is used as the case study

1. One-Dimensional Phase Change

Carslaw and Jaeger (1959) and Ku and Chan (1990) analysed and obtained exact solutions of 1D phase change of a semi-infinite slab as shown in Appendix A. Hence, the 1D validation test case involves a long slab that with no heat transfer at the far end during the considered time domain. The descriptions of the problem are as follows. A 4-m slab has initial temperature T_i = 10ºC. The boundary condition at one end is constant temperature T_C = −20ºC while there is no heat flux at the other end as illustrated in Figure 3. Uniform control volumes with size x are used.

Specified material properties in solid and liquid phases are shown in Table 2. Others are freezing temperature T_F = 0ºC and latent heat for solidification L = 338 kJ/kg. As the convection of the water across cell faces and the induced stress due to the expansion of the ice are not included in this study, the density of the ice is approximated to that of the water to ensure the conservation of mass

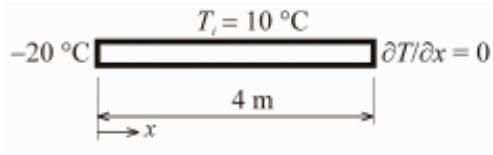

Figure 3. 1D problem descriptions at t = 0 s.

Table 2. 1D case: specified material properties.

Properties	Liquid	Solid
k (W/m·K)	0.556	2.220
c (kJ/kg·K)	4.226	1.762
ρ (kg/m^3)	1000	1000

of each control volumes. When the approximations of k_{INT} are considered, values of different k_{INT} are k_S = 2.220 W/m·K, arithmetic mean k_{ARITH} = 1.388 W/m·K and harmonic mean k_{HAR} = 0.889 W/m·K.

A grid and time step independent model, consisting of 400 cells (x = 0.01 m) and t = 10 s, is employed. Figure 4 shows the comparisons between the analytical temperature and numerical results of simulations with explicit scheme and various k_{INT} at time instant t = 5, 20, 40, and 80 h. The temperature distributions show that liquid cells cool down slowly due to low diffusivity $\alpha = k/\rho c$ and low temperature gradient. Once a control volume is frozen, its temperature drops rapidly such that the temperature gradient in the ice is almost linear. This clearly illustrates that the rate of heat transfer is predominantly controlled by the position of the freezing front. As ice is a good insulator, the freezing front advances at ever slowing rate.

It is found that under the same interface approximation, the resulting temperature from the explicit, Crank-Nicolson and fully implicit time-stepping schemes have similar values once cell size and time step independencies are obtained as examplified by the maximum errors of temperature at time t = 20 h in Figure 5.

On the other hand, the interface conductivity k_{INT} significantly influences the numerical results. The maximum temperature errors from explicit calculations at different time instants are shown in Figure 6. For all interface approximations, the maximum errors occur near the edge of the slab in early time steps due to high temperature gradients in this region at that time. The k_S approximation yields best numerical results with slight overestimation, which corresponds with the physical meanings described previously. Meanwhile, values of the k_{ARITH} and k_{HAR} are much lower than k_S, resulting in less heat flux leaving the saturated control volume across the cell face. Simulations, henceforth, show lower frozen rates accordingly. The k_{HAR}, which is recommended for interfaces of two different materials, performs especially badly as the freezing front, whose movement continuously increases the conductivity in saturated cells.

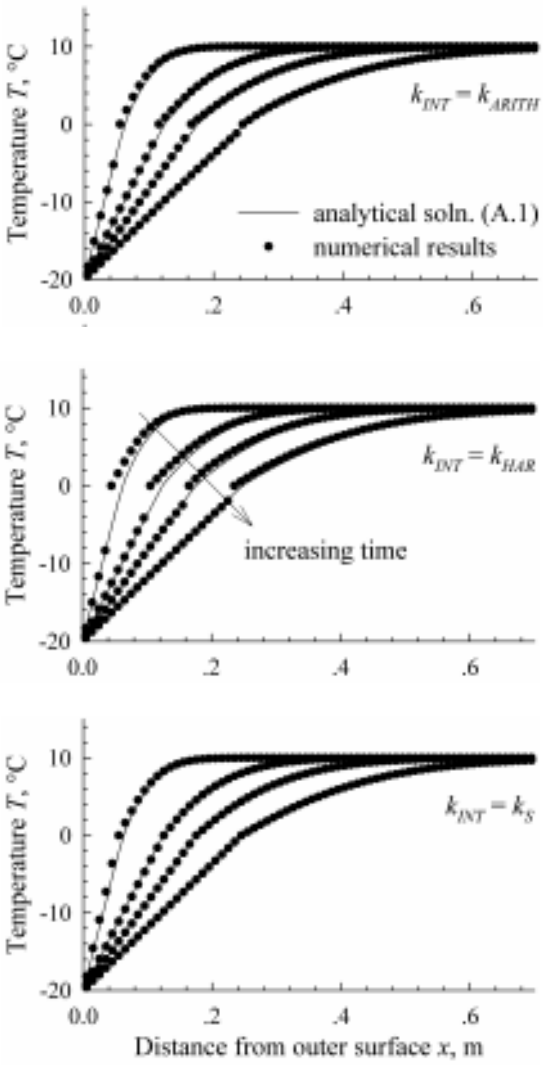

Figure 4. 1D case: temperature from different k_{INT} at t = 5, 20, 40 and 80 h.

When the grid and time step dependencies are considered, it is found that the grid dependency can be obtained with the use of x = 0.01 m, equivalent to the total of 400 cells. More interest-

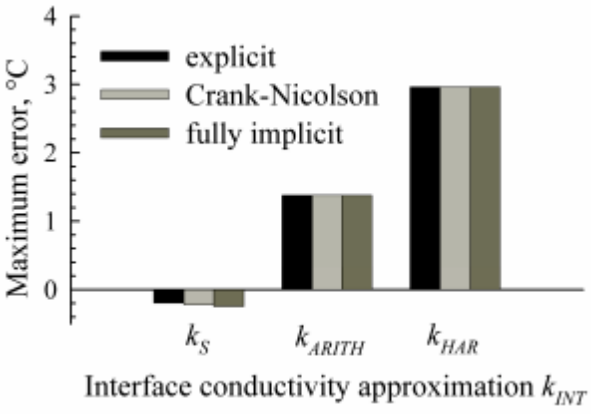

Figure 5. 1D case: maximum errors of temperature from different k_{INT} at t = 20 h.

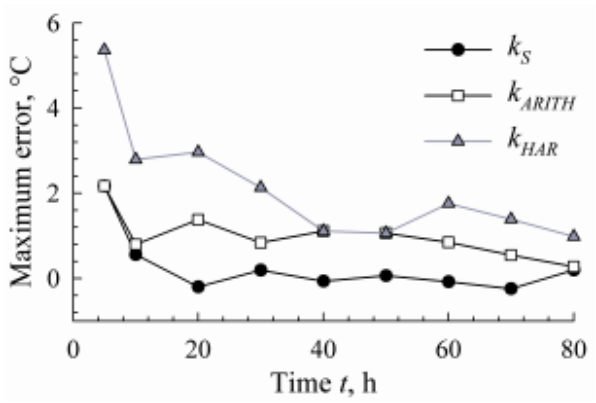

Figure 6. 1D case: maximum errors of temperature from explicit models with different k_{INT}.

ing is the additional restriction of time step sizes t. The maximum errors the required CPU times from simulations with various t at t = 5 h are summarised in Table 3. As previously described, explicit scheme has a restriction on time step size, and large time intervals cause the solutions to diverge. Crank-Nicolson and fully implicit schemes may employ somewhat larger time steps but the accuracy still depends on time step sizes. In addition, implicit schemes require more CPU time than the explicit scheme due to the iterative procedures of the solver.

Moreover, the number of saturated cells on the freezing front at a given instant varies according to the size of time step. Figure 7 compares fully implicit results from a model consisting of 400

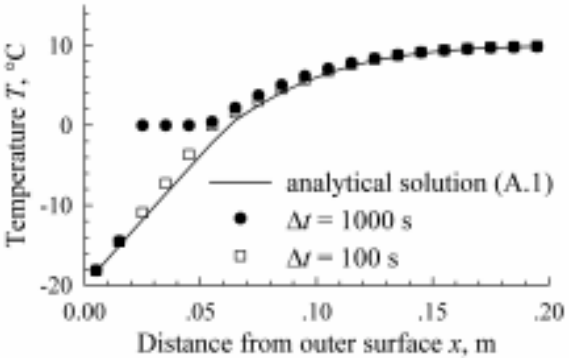

Figure 7. 1D case: comparison of temperature with different t.

cells with $k_{INT} = k_{INT}$ with different t. When the large time step size is used, several nodes undergo

Table 3. 1D case: maximum errors of temperature and CPU time at t = 5 h.

k_{INT}	Scheme	Maximum Error (ºC)				CPU time (s)			
		t = 1000 s	t = 100 s	t = 10 s	t = 1 s	t = 1000 s	t = 100 s	t = 10 s	t = 1 s
k_S	Explicit	diverge	diverge	2.170	2.170	diverge	diverge	3.13	5.77
	Crank-Nicolson	8.579	2.170	2.170	2.170	2.96	3.29	3.41	7.63
	Fully Implicit	11.82	2.170	2.170	2.170	2.97	2.91	3.35	6.97
k_{ARITH}	Explicit	diverge	diverge	2.170	2.170	diverge	diverge	3.84	5.72
	Crank-Nicolson	8.579	2.170	2.170	2.170	2.91	3.13	3.46	7.31
	Fully Implicit	11.82	2.170	2.170	2.170	2.86	2.91	3.24	8.62
k_{HAR}	Explicit	diverge	diverge	5.358	5.358	diverge	diverge	3.24	5.49
	Crank-Nicolson	8.579	5.358	5.358	5.358	2.86	2.85	3.52	7.30
	Fully Implicit	11.82	5.358	5.358	5.358	2.75	3.08	3.35	6.71

the phase change process at a given instant. As the rate of heat transfer is mostly controlled by the freezing front position, the wider the band of saturated control volumes, the lower the heat transfer rate. Thus, there is an additional, but dominating, restriction on step sizes in all time-stepping schemes so that the freezing front is one cell deep.

2. Two-Dimensional Phase Change

The semi-analytical solution of phase change in a semi-infinite region, described in Appendix A, was obtained by Rathjen and Jiji (1971). A region with 8 m × 8 m area is considered. At the initial time t_0, all initial temperatures are T_i = 10ºC. The boundary conditions at edges are T_C = −20ºC. Due to symmetry, only one-fourth of the total area is modelled as shown in Figure 8 with no heat flux across the surfaces *BC* and *CD*.

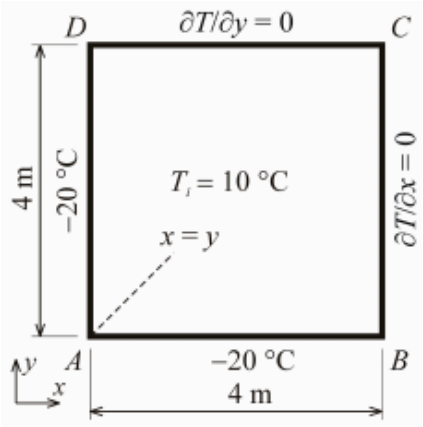

Figure 8. 2D case: problem descriptions.

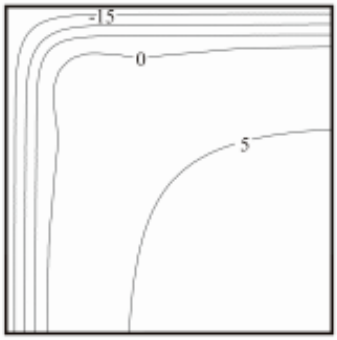

Figure 9. 2D case: analytical temperature contours (ºC) at t = 20 h.

Specified material properties are freezing temperature T_F = 0ºC and latent heat for solidification = 338 kJ/kg. Since the existing solution specifies the same thermal diffusivity α for both liquid and solid phases, the properties for both phases are given as conductivity k = 2.220 W/m·K, specific heat c = 1.762 kJ/kg·K and density ρ = 1000 kg/m^3. Hence, the approximation of interface conductivity is not considered in this case. The analytical temperature contour at t = 20 h are shown in Figure 9.

The uniform 400×400 control volumes (Δx = Δy = 0.01 m) are used to model the domain while time step Δt = 10 s. Numerical results from all three time-stepping schemes are found to be similar and agree well with the analytical solution. Thus, only explicit results along the line $x = y$ at time instants t = 5, 20, 40 and 80 h, shown in Figure 10, are used as the representative in the comparison with the analytical solutions.

The temperature distributions clearly show heat transfer through both exposed edges, causing a parabolic temperature profile instead of a linear one as in 1D case. As diffusivity in both phases is equal for this problem, the rate of heat transfer depends solely on the temperature gradient, which is dominated by the freezing front position.

The maximum errors of temperature and required CPU times at t = 5 h are summarised in Table 4. Even more apparent than in 1D, implicit schemes require more computational time due to the iterative procedures of the solver. Hence, the CPU time superiority of the explicit scheme for this phase change problem is apparent.

Three grids are employed in the consideration of grid dependency. The coarse mesh contains 100×100 cells (Δx = Δy = 0.04 m) and is successively refined to grids of 200×200 and 400×400 cells. The explicit results of these grids with Δt = 10 s at t = 5 h are shown in Figure 11. As expected, finer grids yield more accurate solutions. Nonetheless, the results from coarsest grid do follow the analytical trend quite well.

Figure 12 compares fully implicit results

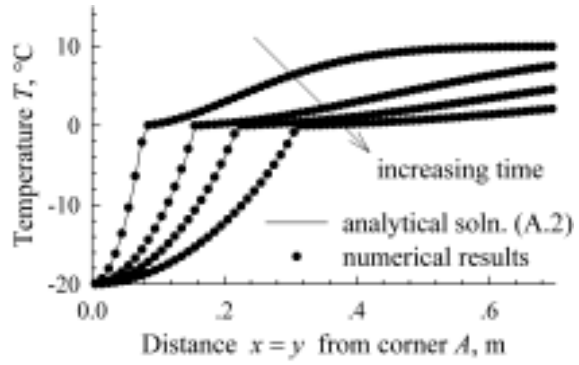

Figure 10. 2D case: temperature profile from explicit scheme at t = 5, 20, 40 and 80 h.

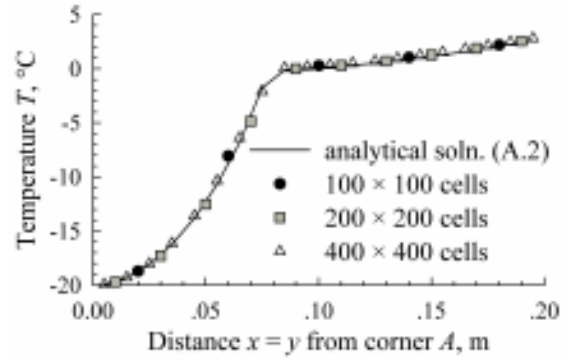

Figure 11. 2D case: temperature comparisons for the evaluation of grid dependency.

between t = 1000 s and 100 s in the study of time interval sizes for the grid with 400×400 cells. The observations regarding the number of nodes undergoing phase change at the same time in the 1D case is also applicable and even more significant in the 2D cases.

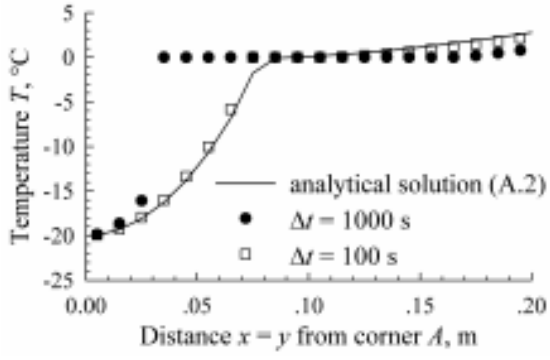

Figure 12. 2D case: comparison of temperature with different t.

3. Case Study

The developed program is employed to study the freezing process in industrial ice block manufacturing with conditions taken from a manufacturer in Pattani (Prapainop, 2002). The cross-sectional area of ice block is 0.52 m × 0.13 m. Initially, temperature of water is T_i = 30ºC throughout. The boundary conditions along the edges are T_C = −10ºC. Due to symmetry, only one-fourth of the total area is modelled as shown in Figure 13. The grid consists of 26×13 cells while t = 10 s. From the results in the previous section, the explicit scheme with $k_{INT} = k_S$ is employed. The real properties of ice and water, as in the 1D validation, are used.

The predicted temperature contours at time t = 5 h are shown in Figure 14 while Figure 15 shows the temperature along the line $x = y$ at t = 1, 2, 3, 4 and 5 h. The history of temperature at the innermost control volume, which freezes last, as well as the position of freezing front along the line $x = y$, is illustrated in Figure 16. It takes around 42

Table 4. 2D case: maximum error of temperature and CPU time at t = 5 h when $k_{INT} = k_S$.

Scheme	Maximum Error (ºC)				CPU time (s)			
	t = 1000 s	t = 100 s	t = 10 s	t = 1 s	t = 1000 s	t = 100 s	t = 10 s	t = 1 s
Explicit	diverge	diverge	0.931	0.931	diverge	diverge	528	5204
Crank-Nicolson	14.16	3.313	1.767	0.931	430	791	3536	22435
Fully Implicit	16.56	4.964	1.767	1.624	541	922	3091	21561

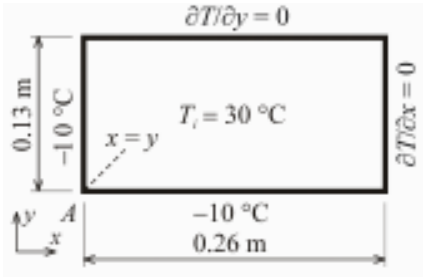

Figure 13. Problem descriptions of the test case.

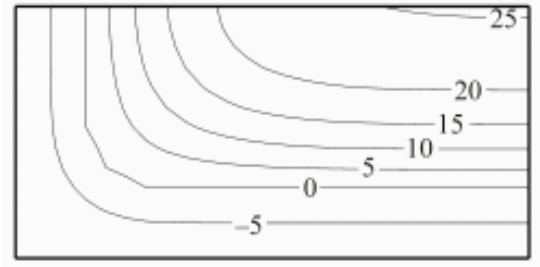

Figure 14. Test case: temperature contours (ºC) at t = 5 h.

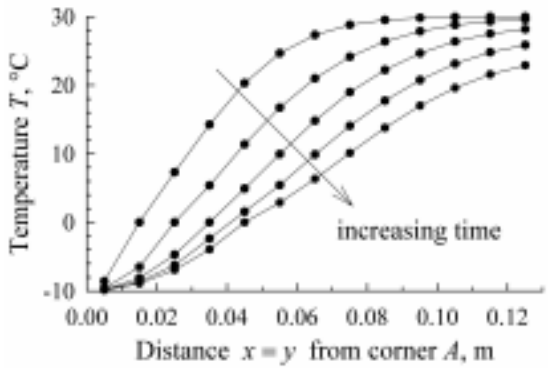

Figure 15. Test case: temperature at t = 1 to 5 h with 1 h increment.

hours for the water to fully freeze, compared to the real manufacturing cycle of 48 hours. In 3D analysis, water is expected to freeze even faster. This tentatively indicates that the manufacturing cycle may be shortened if the boundary temperature can be maintained.

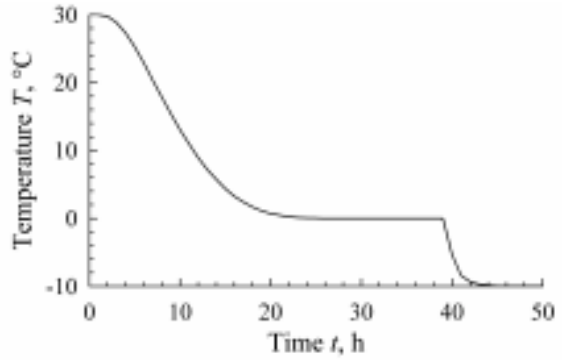

Figure 16. Test case: temperature history of the innermost cell and location of saturated cells.

Conclusions

The ice formation modelling by the finite volume method with the fixed grid and the latent heat by fictitious sensible heat schemes is successfully performed. As the freezing front should be one cell deep, this dominating restriction controls both the time interval and grid sizes in all time-stepping schemes. It is shown that all temporal schemes yield similar results once the grid and time interval independencies are achieved. Hence, it is recommended that the explicit scheme is used as it requires less computational effort. On the other hand, the approximation of interface conductivity strongly influences numerical results. It is found that the use of harmonic mean, recommended for composite materials, yield unsatisfactory results as the freezing front advances through the control volume and the discontinuity does not remain at the cell faces as in composite interfaces. The best numerical solutions are obtained with the approximation of the interface conductivity by the solid conductivity, which slightly overestimates the conductivities as the freezing front progresses across the saturated control volume. Future developments include the modelling of ice expansion, residual stress, varying properties and adaptive grids for moving front, comparisons with measured results as well as industrial applications.

Acknowledgements

The authors would like to thank Assoc. Prof. Manit Thongprasert. The supports from the Thailand Research Fund (TRF) for the Senior Scholar Prof. Pramote Dechaumphai and the Development Grant for New Researcher/Lecturer, Chulalongkorn University are acknowledged.

References

Askar, H.G. 1987 The front tracking scheme for the one-dimensional freezing problem, Int. J. Numer. Methods Eng., 24: 859-869.

Carslaw, H.S. and Jaeger, J.C. 1959. Conduction of Heat in Solids, Clarendon Press, London, 282-295.

Celentano, D., Onate, E. and Oller, S. 1994. A temperature-based formulation for finite element analysis of generalized phase-change problems, Int. J. Numer. Methods Eng., 37: 3441-3465.

Comini, G., Guidice S.D., Lewis, R.W. and Zienkiewicz, O.C. 1974. Finite element solution of non-linear heat conduction problems with special reference to phase change, Int. J. Numer. Methods Eng., 8: 613-624.

Comini, G., Guidice, S.D. and Saro, O. 1990. A conservative algorithm for multidimensional conduction phase change, Int. J. Numer. Methods Eng., 30: 697-709.

Crivelli, L.A. and Idelsohn, S.R. 1986. A temperature-based finite element solution for phase-change problems, Int. J. Numer. Methods Eng., 23: 99-119.

Dalhuijsen, A.J. and Segal, A. 1986. Comparison of finite element techniques for solidification problems, Int. J. Numer. Methods Eng., 23: 1807-1829.

Dhatt, G., Song, R. and Cheikh, A.N. 1989. Direct enthalpy method for solidification calculation, in Gruber, R. *et al*. (eds.), Prods. of the Fifth Int. Symp. on Numerical Methods in Engineering, Boston, 487-494.

Guidice, S.D., Comini, G. and Lewis, R.W. 1978. Finite element simulation of freezing process in soils, Int. J. Numer. Anal. Methods Geomech., 2: 223-235.

Kim, C.-J. and Kaviany, M. 1990. A numerical method for phase change problems, Int. J. Heat Mass Transfer, 33: 2721-2734.

Ku, J.Y. and Chan, S.H. 1990. A generalized Laplace transform technique for phase-change problems, J. Heat Transfer, 112: 495-497.

Lemmon, E.C. 1979. Phase change techniques for finite element codes. in Lewis, R.W. and Morgan, K. (eds.), Numerical Methods in Thermal Problems, Swansea, 149-158.

Morgan, K., Lewis, R.W. and Zienkiewicz, O.C. 1978. An improved algorithm for heat conduction problems with phase change, Int. J. Numer. Methods Eng., 12: 1191-1195.

Murray, W.D. and Landis, F. 1959. Numerical and machine solutions of transient heat conduction problem involving melting or freezing, J. Heat Transfer, 81: 106-112.

Patankar, S. 1980. Numerical Heat Transfer and Fluid Flow, Hemisphere Publishing Corporation, New York.

Pham, Q.T. 1986. The use of lumped capacitance in the finite-element solution of heat conduction problems with phase change, Int. J. Heat Mass Tran., 29: 285-291.

Prapainop, R. 2002. Simulation of Ice Formation by Finite Volume Method, M.Eng. Thesis, Department of Mechanical Engineering, Chulalongkorn University.

Rathjen, K.A. and Jiji, L.M. 1971. Heat conduction with melting or freezing in a corner, J. Heat Transfer, 93: 101-109.

Rolph III, W.D. and Bathe, K.J. 1982. An efficient algorithm for analysis of nonlinear heat transfer with phase changes, Int. J. Numer. Methods Eng., 18: 119-134.

Roose, J. and Storrer, O. 1984. Modelization of phase changes by fictitous heat flow, Int. J. Numer. Methods Eng., 20: 217-225.

Rubinsky, B. and Cravahlo, E.G. 1981. A finite element method for the solution of one-dimensional phase change problems, Int. J. Heat Mass Tran., 24: 1987-1989.

Tamma, K. and Namburu, R. 1990. Recent advances, trends and new perspective via enthalpy-based finite element formulations for applications to solidification problems, Int. J. Numer. Methods Eng., 30: 803-820.

Thomas, B.G., Samarasekera, I.V. and Brimacombe, J.K. 1987. Mathematical model of the thermal processing of steel ingots: part I, heat flow model, Metall. Trans. B., 18: 119-130. cited in Reddy, M.P. and Reddy, J.N. 1992. Numerical simulation of forming processes using a coupled fluid flow and heat transfer model, Int. J. Numer. Methods Eng., 35: 807-833.

Versteeg, H.K. and Malalasekera, W. 1995. An Introduction to Computational Fluid Dynamics: The Finite Volume Method, Longman Scientific & Technical, England.

Voller, V. and Cross, M. 1981. Accurate solutions of moving boundary problems using the enthalpy method, Int. J. Heat Mass Tran., 24: 545-56.

Voller, V. and Cross, M. 1983. An explicit numerical method to track a moving phase change front, Int. J. Heat Mass Tran., 26: 147-150.

Voller, V., Swaminathan, C.R. and Thomas, B.G. 1990. Fixed grid techniques for phase change problems: a review, Int. J. Numer. Methods Eng., 30: 875-898.

Weaver, J.A. and Viskanta, R. 1986. Freezing of liquid-saturated porous media. J. Heat Mass Transfer, 33: 2721-2734.

Appendix A: Analytical Solutions

The exact solutions for the 1D and 2D phase change validation in section 4 are roughly described in this appendix. It is recommended that the original articles are consulted for full descriptions.

1. One-Dimensional Phase Change

Exact solutions of 1D phase change of a semi-infinite slab were analysed by Carslaw and Jaeger (1959) and Ku and Chan (1990) with the moving front approach. The exact temperature distributions in solid, T_S, and liquid, T_L, respectively are:

$$T_S = T_C + (T_F - T_C)\frac{\mathrm{erf}(x^*)}{\mathrm{erf}(x^*_{SL})} \qquad \text{when } 0 < x^* < x^*_{SL},$$

$$T_L = T_i + (T_F - T_i)\frac{\mathrm{erfc}(\sqrt{\alpha_S / \alpha_L x^*})}{\mathrm{erfc}(\sqrt{\alpha_S / \alpha_L x^*_{SL}})} \qquad \text{when } x^*_{SL} < x^* < \infty, \tag{10}$$

where $x^* = x / 2\sqrt{\alpha_S t}$ is the dimensionless position and $\alpha = k/\rho c$ is the thermal diffusivity which are calculated from corresponding mechanical properties for both solid α_S and liquid α_L values. The values of dimensionless position of solid-liquid interface x^*_{SL} are obtained via the nonlinear algebraic equation:

$$\frac{T_F - T_i}{T_F - T_C}\frac{k_L}{k_S}\sqrt{\frac{\alpha_S}{\alpha_L}}\frac{\exp(-(\alpha_S/\alpha_L)(x^*_{SL})^2)}{\mathrm{erfc}(\sqrt{\alpha_S/\alpha_L}\,x^*_{SL})} + \frac{\exp(-(x^*_{SL})^2)}{\mathrm{erf}(x^*_{SL})} - \frac{\sqrt{\pi}x^*_{SL}L}{c_S(T_F - T_C)} = 0. \tag{11}$$

2. Two-Dimensional Phase Change

Rathjen and Jiji (1971) present an analytical solution to the two-dimensional free boundary problem of solidification in a semi-infinite region subjected to a constant wall temperature. The exact solution takes the form of dimensionless temperature field $T^* = T^*_S = (T_S - T_F)/(T_F - T_C)$ in the solid domain and $T^* = T^*_L = k_L(T_L - T_F)/k_S(T_F - T_C)$ in the fluid domain as $T^* = U + V$. The solution to the heat conduction U is a function of dimensionless position $x^* = x / 2\sqrt{\alpha t}$ and $y^* = y / 2\sqrt{\alpha t}$ as:

$$U = -1 + (1 + T^*_i)\mathrm{erf}(x^*)\mathrm{erf}(y^*), \tag{12}$$

where dimensionless initial temperature $T^*_i = (T_i - T_F)/(T_F - T_C)$. The function V involves the phase change and is obtained by Gaussian integration of function:

$$V = \frac{\beta}{2\pi}\int_0^1\int_{x_0^*}^{\Lambda}\left[f(\eta)-\eta\frac{df(\eta)}{d\eta}\right]\times$$

$$\left[K(\eta,\tau;x^*)K(f(\eta),\tau;y^*)+K(f(\eta),\tau;x^*)K(\eta,\tau;y^*)\right]d\eta\frac{d\tau}{1-\tau}+$$

$$\frac{\beta\lambda}{4\pi^{1/2}}\int_0^1\left[K(\lambda,\tau;y^*)E(\tau;\Lambda;x^*)+K(\lambda,\tau;x^*)E(\tau;\Lambda;y^*)\right]\frac{d\tau}{\tau^{1/2}(1-\tau)^{1/2}}, \quad (13)$$

where $\beta = L/c_S(T_F - T_C)$ is the latent to sensible heat ratio, x_0^* is the intersection of solidification front f and $x^* = y^*$ and Λ and λ are related positions in the dimensionless domain as shown in Figure 17. The dimensionless integration variables η is for x^* and τ for time while functions are:

$$K(\eta,\tau;x^*) = \exp\left[\frac{-(x^*-\tau^{1/2}\eta)^2}{1-\tau}\right]-\exp\left[\frac{-(x^*+\tau^{1/2}\eta)^2}{1-\tau}\right], \quad (14)$$

$$E(\tau;\Lambda;x^*) = \mathrm{erf}\left[\frac{x^*-\Lambda\tau^{1/2}}{(1-\tau)^{1/2}}\right]-\mathrm{erf}\left[\frac{x^*+\Lambda\tau^{1/2}}{(1-\tau)^{1/2}}\right], \quad (15)$$

$$f(x^*) = \left[\lambda^m+\frac{C}{(x^*)^m-\lambda^m}\right], \quad (16)$$

where m and C are numerically determined constants.

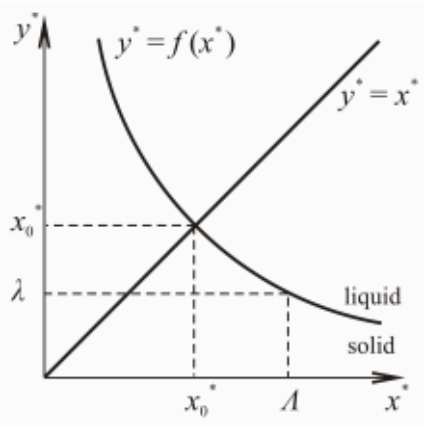

Figure 17. Diagram of dimensionless variables for the exact solution of 2D phase change